

Data Release for the low-energy event study in the HVeV detector

SuperCDMS Collaboration

June 28, 2022

This document accompanies the public release of data used in the SuperCDMS-HVeV paper on the investigation of the sources of low-energy events [1]. The provided data and information allow the community to use these data for their own analyses or for reproducing the results, published in the paper. Questions about this release should be directed to supercdms_publications@lists.astro.caltech.edu.

The provided experimental and supplemental data files are described in Sec. 1. The limit setting procedure is described in Sec. 2.

1 Description of the files

This data release includes two folders with data files, described in the following subsections, and a Jupyter notebook `make_plots.ipynb` that can be used to reproduce figures 1, 3, 4, 5, 14, 15 and 16 from the original paper [1]. The only required packages to run the notebook are `numpy` and `matplotlib`.

1.1 `limit_data` folder

The `limit_data` folder contains the data, required to reproduce the spin-independent dark matter-nucleon scattering cross-section limit, presented in the original paper [1]. This subsection describes the content of the files. The limit-setting procedure is described in more detail in Sec. 2.

- `spectrum_before_cuts.tsv`: reconstructed energies of events observed in the experiment with 0 V voltage before data quality selections in the unit of eV.
- `spectrum.tsv`: reconstructed energies of events observed in the experiment with 0 V voltage after data quality selections in the unit of eV.
- `efficiency.txt`: data quality selection efficiency. First column — recoil energy in the unit of eV; second column — corresponding data-quality cuts efficiency; third and fourth columns — lower and upper bound of the efficiency statistical uncertainty; fifth column — fit to the efficiency with an energy-independent model; sixth column — 1σ statistical uncertainty on the fit.
- `signal_model_dm_masses.tsv`: list of dark matter (DM) masses in the unit of MeV/c^2 , corresponding to the columns in `signal_models.tsv` and `signal_models_scaled.tsv`.
- `signal_models.tsv`: DM signal model differential rates with the detector response taken into account: the first column is the recoil energy in keV, the rest of the columns are the differential rates in the unit of $1/\text{keV}/\text{kg}/\text{day}$ for the DM masses, specified in the `signal_model_dm_masses.tsv` list.
- `signal_models_scaled.tsv`: same as the `signal_models.tsv`, but with the rescaled energy calibration. Used to estimate the systematic uncertainty on the limit.
- `no_shielding_limit.tsv`: 90% confidence level (C.L.) exclusion limit on the spin-independent DM-nucleon scattering cross section with the systematic uncertainty, originated from the energy calibration uncertainty. First column — DM mass in MeV/c^2 ; second column — limit cross section in cm^2 ; third

column — upper bound of the limit systematic uncertainty in cm^2 . The lower bound coincides with the nominal value, provided in the second column. All the values are rounded to 9 significant figures.

- `limit_with_upper_bound_from_shielding.tsv`: spin-independent DM-nucleon scattering cross section exclusion region with an upper bound calculated, originated from the atmosphere and Earth shielding effect. First column — DM mass in MeV/c^2 ; second column — lower bound of the cross section exclusion limit in cm^2 ; third column — upper bound of the cross section exclusion limit in cm^2 . All the values are rounded to 9 significant figures.
- `verne_output/N_OVeV_lmxX.txt`: 29 files, containing the expected DM event counts as functions of DM-nucleon scattering cross section σ_N^{SI} with the atmosphere and Earth shielding taken into account. X in the filename should be replaced with $\log_{10}(m_{\text{DM}}/(\text{MeV}/c^2))$, where m_{DM} is the corresponding DM mass in the unit of MeV/c^2 . The first column in each file is the logarithm of the cross section $\log_{10}(\sigma_N^{\text{SI}}/\text{cm}^2)$. The second column is the expected number of DM events that would be observed in the given experiment with the given signal model.

1.2 data_files folder

The `data_files` folder contains the data used for the calibration and the energy spectra study of background events in the HVeV detector. Data of each figure are in a folder named `fig#`, where `#` is the figure number in Ref. [1].

1.2.1 fig1 folder

This folder contains three comma-delimited txt files, which provide the data needed to create Fig. 1. Each file has a different format, due to the nature of the data. The explanation is below.

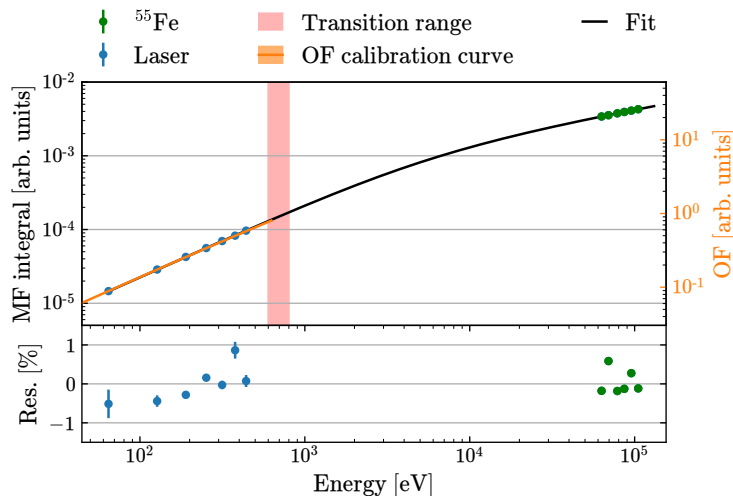


Figure 1: (Figure 1 of Ref. [1]) Top: Application of the energy calibration curve. The MF integral calibration curve (black) and a representative example of the OF calibration curve from Fe-day (orange, corresponds to Eq. 1 in the original paper). The OF calibration curve includes an $\sim 11\%$ systematic uncertainty band, and corresponds to the y-axis on the right side. The vertical red shaded region marks the 600–800 eV transition range. Bottom: residuals between the data points and the calibration curve expressed in percentage.

- `MF_calib_points.txt`: This file contains the calibration points for the MF energy estimator from the laser and ^{55}Fe data. The first column is a list of the nominal energy in the unit of eV (x axis in Fig 1). The second column is the value of MF energy estimator (y axis in Fig 1). The third column is the uncertainty of the MF energy estimator. The fourth column is the fit residual in the unit of percentage.

In each column the first seven rows are from the laser data, while the rest of the rows are from the ^{55}Fe data.

- `MF_calib_curve.txt`: This file contains the parameters for the calibration curve of the MF energy estimator. These parameters are the coefficients of a 4th order polynomial $a_4 * x^4 + a_3 * x^3 + a_2 * x^2 + a_1 * x^1 + a_0$. The numbers from left to right correspond to $a_4 - a_0$.
- `OF_calib_curve.txt`: This file contains the parameters for the calibration curve of the OF energy estimator. Numbers are the coefficients of a 2nd order polynomial $ax * (1 + b * x)$. The first number is a, and the second number is b.

1.2.2 fig14 folder

This folder contains one comma-delimited txt file, which is the selection efficiency of 0V data for the background study.

- `burst_efficiency.txt`: This file has data points of the efficiency for burst event study. The first column is a list of energies in the unit of eV. The second to fourth columns are the center value and lower/upper bound of the selection efficiency calculated from laser data. The fifth to seventh columns are the center value and lower/upper bound of the selection efficiency calculated from the burst event simulation. The last three columns are the center value and lower/upper bound of the combined selection efficiency.

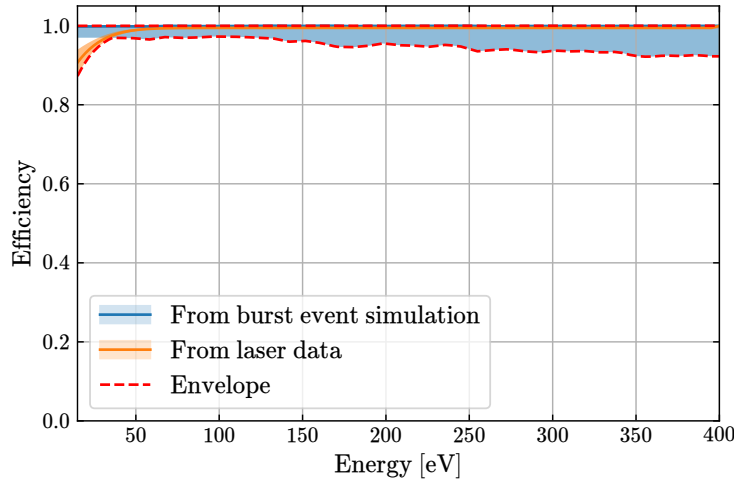


Figure 2: (Figure 14 of Ref. [1]) 0 V data selection efficiencies evaluated with laser calibration data (orange) and burst event simulation (blue), and associated uncertainties (shading). The dashed red lines are the envelope of the two uncertainty bands, which is used as the total uncertainty of the selection efficiency.

1.2.3 fig15 folder

This folder contains five comma-delimited txt files. Four of them are the response matrices with different settings in burst event simulation. The last one is a list of energy that the matrix components correspond to.

- `Nominals.txt`: The response matrix from the burst event simulation with nominal settings. The horizontal direction corresponds to the reconstructed energy of HV events, and the vertical direction corresponds to the reconstructed energy of 0V events. The energy that the i^{th} row/column corresponds to is recorded in `xbincenters.txt`.

- `No_Secondary_pulses.txt`: The response matrix from the burst event simulation with no secondary pulses. File structure is the same as above.
- `Secondary_pulses_x0.5.txt`: The response matrix from the burst event simulation with half of the secondary pulses. File structure is the same as above.
- `Secondary_pulses_x2.txt`: The response matrix from the burst event simulation with twice the secondary pulses. File structure is the same as above.
- `xbincenters.txt`: This file is a list of energy that the i^{th} row/column of the response matrix corresponds to.

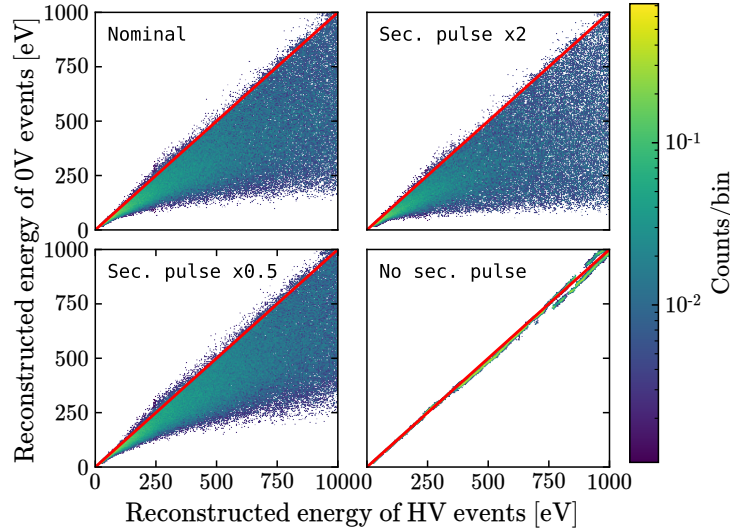


Figure 3: (Figure 15 of Ref. [1]) Response matrices that convert the 100 V spectrum to 0 V assuming $\epsilon_{\text{eff}} = 4\text{eV}$. The four panels correspond to different settings for the rate of secondary pulses in the burst event simulation.

1.2.4 fig16 folder

This folder contains six comma-delimited txt file, which are the recoil energy and phonon energy spectra of the 0 V, 60 V and 100 V background exposure.

- `phonon_energy_0.V.txt`: Phonon energy spectrum of the 0 V data. The first column is the energy bin center. The second column is the bin counts.
- `phonon_energy_60.V.txt`: Phonon energy spectrum of the 60 V data. File structure is the same as above.
- `phonon_energy_100.V.txt`: Phonon energy spectrum of the 100 V data. File structure is the same as above.
- `recoil_energy_0.V.txt`: Recoil energy spectrum of the 0 V data. The first column is the energy bin center. The second column is the bin counts. The third column is the uncertainty of the bin counts.
- `recoil_energy_60.V.txt`: Recoil energy spectrum of the 60 V data. File structure is the same as above.
- `recoil_energy_100.V.txt`: Recoil energy spectrum of the 100 V data. File structure is the same as above.

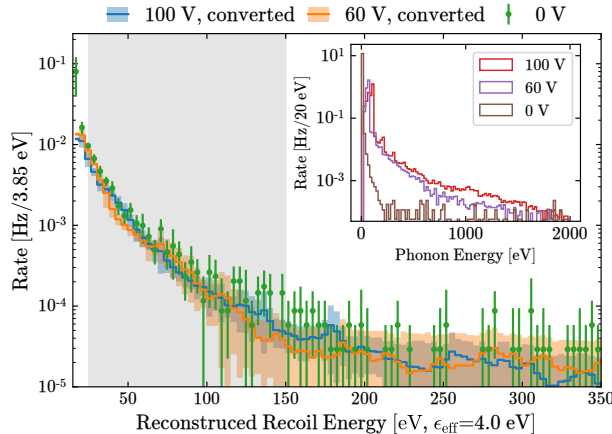


Figure 4: (Figure 16 of Ref. [1]) Comparison of the converted HV spectra with the 0V spectrum. The gray area shows the energy range (25-150 eV) where the χ^2 is calculated. The inset plot shows the phonon spectra before applying the response matrix conversion.

2 Limit Setting

An exclusion limit on the spin-independent dark matter-nucleon scattering cross section was obtained using the experimental data that can be found in the `limit_data/spectrum.tsv` file. The file contains energies of the events that passed the live-time and data quality selections. The science exposure is 0.185 gram-days. The energy region of interest (ROI) spans an interval from the trigger threshold (9.2 eV) to the cut-off value of 250 eV. The energy spectrum before and after the data-quality selections is shown on Fig. 5. An energy-independent model for the data-quality selection efficiency was used (Fig 6).

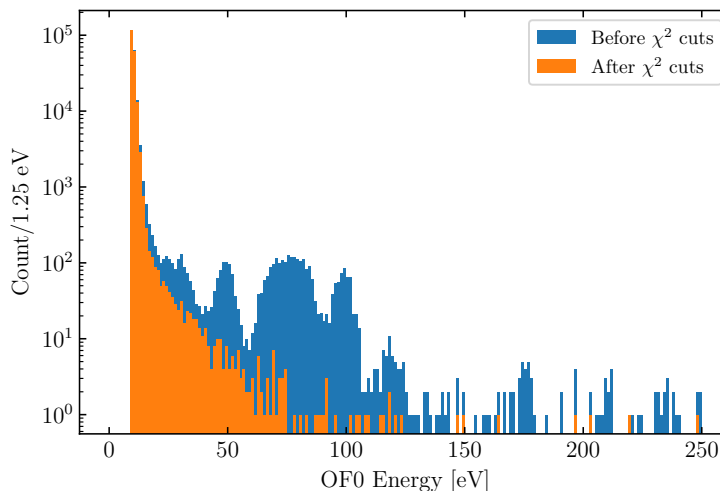


Figure 5: (Figure 3 of Ref. [1]) Experimental energy spectrum before and after the data-quality selections.

The standard WIMP signal model [2] with the following parameters was used: an asymptotic value of the Maxwellian velocity distribution $v_0 = 220$ km/s, a galactic escape velocity $v_{\text{esc}} = 544$ km/s, a local DM mass density $\rho_0 = 0.3 \text{ GeV}/(c^2 \cdot \text{cm}^3)$ and a mean orbital velocity of the Earth $v_{\text{lab}} = 232$ km/s [3, 4, 5]. The differential rates for various dark matter mass hypotheses were convolved with the detector response functions, as described in the paper. The resulting differential event rates can be found in the `limit_data/signal_models.tsv` file, with the corresponding dark matter masses in the `limit_data/signal_model_dm_masses.tsv` file.

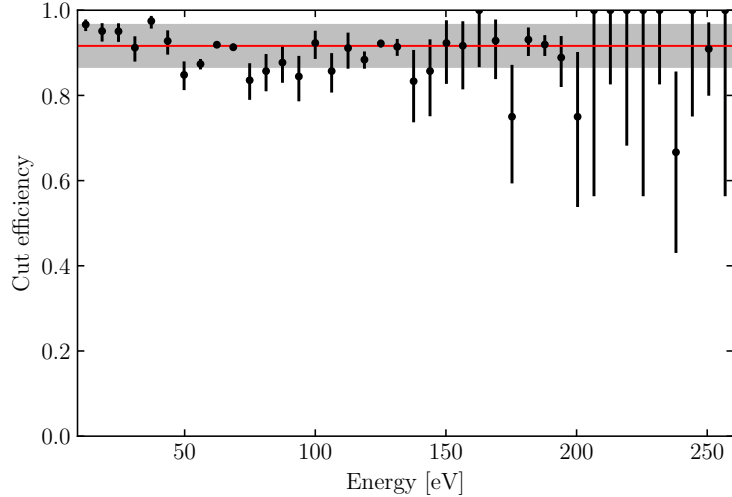


Figure 6: (Bottom panel of Figure 4 of Ref. [1]) Data-quality selection efficiency versus total phonon energy (black data points) fitted with an energy-independent model (red line) with the 1σ -statistical uncertainty (gray band).

To produce the 90% C.L. limit on the DM-nucleon scattering cross section (Fig. 7) the Optimum Interval (OI) [6, 7] method was used. The resulting limit can be found in the `limit.data/limit.tsv` file.

The dominant source of uncertainty in this analysis is the uncertainty on the energy calibration. As described in the paper, an 11% calibration rescaling was used to produce the upper bound of the uncertainty band shown as a shaded area on Fig. 7. To reproduce it the event energies should be multiplied by a factor of 1.11. The signal models should be convolved with the rescaled detector response functions. The results of these convolutions can be found in the `limit.data/signal_models_scaled.tsv` file.

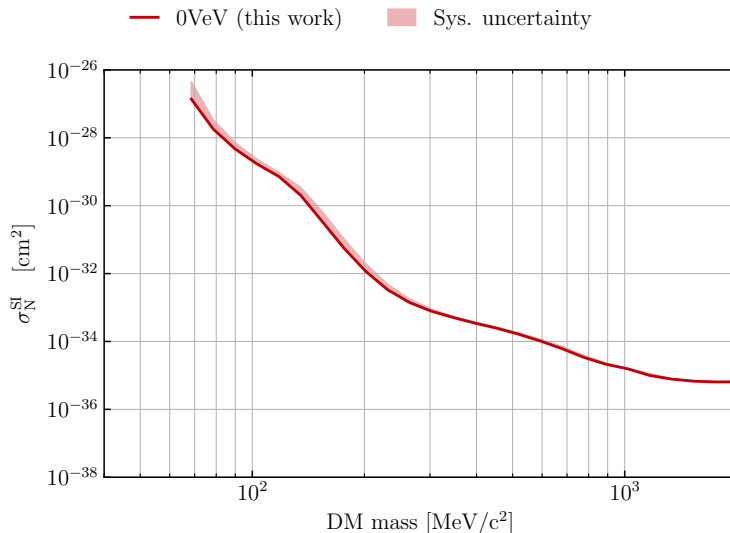


Figure 7: (Left panel of Figure 5 of Ref. [1]) 90% C.L. exclusion limit on the spin-independent DM-nucleon scattering cross section with a systematic uncertainty shown as a shaded area.

To account for the atmosphere and Earth shielding, `verne` package [8] was used, which takes into account the mean direction of the DM flux at the location and the time of the experiment and estimates the impact

of shielding on the Standard Halo Model velocity distribution. A private fork of the version v1.1 of the package was used, with the following changes and configurations:

- asymptotic value of the Maxwellian velocity distribution: 220 km/s;
- galactic escape velocity: 544 km/s;
- detector location: +42.050° N, -87.680° W;
- start of data taking: 18:50, May 11, 2019;
- end of data taking: 5:20, May 12, 2019;
- overburden: 0 meter water equivalent (surface experiment);
- shielding: 15 mm Al;
- exposure, energy ROI, efficiency, detector response functions: described earlier in this note and in the paper.

As an output the expected DM counts in the energy ROI as functions of the cross section were obtained for a range of DM masses (files in the `limit_data/verne_output` folder). The expected event counts are compared to the observed event count, corrected to get the 90% C.L. (195651.255 90% C.L. events for 195084 observed events). The cross section values at which the modelled event counts become smaller than the observed event count defines the upper bound for the cross section exclusion region, as shown on Fig. 8. For the DM masses lower than $92 \text{ MeV}/c^2$ the expected event count never exceeds the observed count, meaning that for these DM masses there are no cross section values which can be excluded by this analysis. This explains the low-mass sharp cut-off in the exclusion region on Fig. 9.

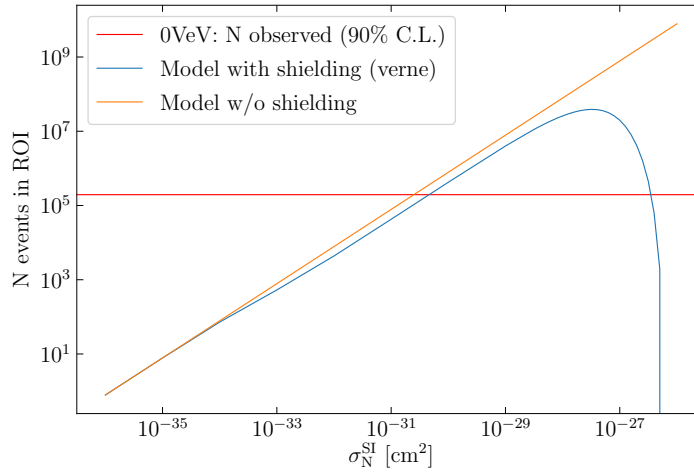


Figure 8: Comparison of the observed and expected event counts in the 0VeV energy ROI for a DM mass equal to $200 \text{ MeV}/c^2$ as a function of DM-nucleon scattering cross section. At some low cross section value, as the shielding effect becomes negligible, the signal models with and without shielding become comparable. The right-most intersection between the shielded signal model and the observed counts defines the upper bound of the exclusion region.

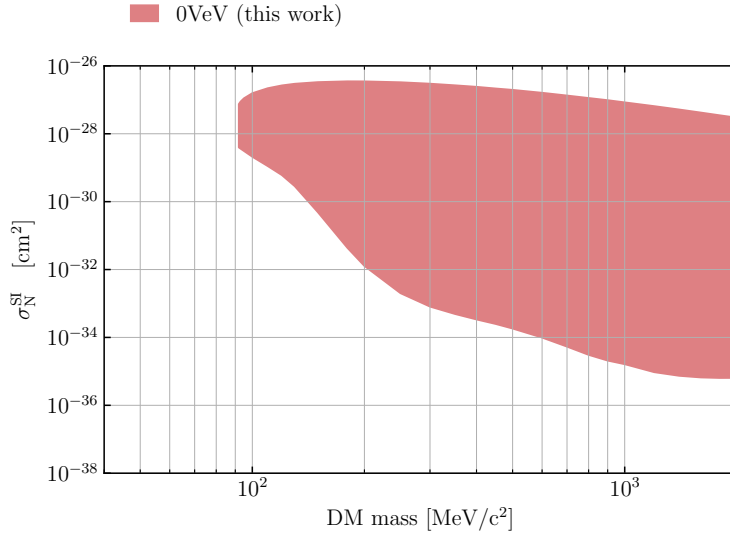


Figure 9: (Right panel of Figure 5 of Ref. [1]) 90% C.L. exclusion region on the spin-independent DM-nucleon scattering cross section. The upper bound is due to the atmosphere and Earth shielding.

References

- [1] M. Albakry et al., Phys. Rev. D **105**, 112006 (2022).
- [2] Z. Ahmed *et al.* (CDMS Collaboration), Phys. Rev. D **83**, 112002 (2011).
- [3] F. J. Kerr and D. Lynden-Bell, Mon. Not. Roy. Astron. Soc. **221**, 1023 (1986).
- [4] M. C. Smith, G. R. Ruchti, A. Helmi, R. F. G. Wyse, J. P. Fulbright, K. C. Freeman, J. F. Navarro, G. M. Seabroke, M. Steinmetz, M. Williams, *et al.*, Mon. Notices Royal Astron. Soc. **379**, 755 (2007).
- [5] R. Schönrich, J. Binney, and W. Dehnen, Mon. Notices Royal Astron. Soc. **403**, 1829 (2010).
- [6] S. Yellin, Phys. Rev. D **66**, 032005 (2002).
- [7] S. Yellin, ArXiv:0709.2701 (2007).
- [8] B. Kavanagh, Phys. Rev. D **97**, 123013 (2017).